Entropy production in chemically nonequilibrium quark-gluon plasma created in central Pb + Pb collisions at energies available at the CERN Large Hadron Collider

V. Vovchenko,[1,2,3] M. I. Gorenstein,[1,4] L. M. Satarov,[1,5] I. N. Mishustin,[1,5] L. P. Csernai,[6] I. Kisel,[1,2] and H. Stöcker[1,2,7]

[1]*Frankfurt Institute for Advanced Studies, D-60438 Frankfurt am Main, Germany*

[2]*Johann Wolfgang Goethe Universität, D-60438 Frankfurt am Main, Germany*

[3]*Taras Shevchenko National University of Kiev, 03022 Kiev, Ukraine*

[4]*Bogolyubov Institute for Theoretical Physics, 03680 Kiev, Ukraine*

[5]*National Research Center "Kurchatov Institute", 123182 Moscow, Russia*

[6]*Institute for Physics and Technology, University of Bergen, 5007 Bergen, Norway*

[7]*GSI Helmholtzzentrum für Schwerionenforschung GmbH, D-64291 Darmstadt, Germany*

We study the possibility that partonic matter produced at an early stage of ultrarelativistic heavy-ion collisions is out of chemical equilibrium. It is assumed that initially this matter is mostly composed of gluons, but quarks and antiquarks are produced at later times. The dynamical evolution of partonic system is described by the Bjorken-like ideal hydrodynamics with a time-dependent quark fugacity. The results of this model are compared with those obtained by assuming the complete chemical equilibrium of partons already at the initial stage. It is shown that in a chemically nonequilibrium scenario the entropy gradually increases, and about 25% of the total final entropy is generated during the hydrodynamic evolution of deconfined matter. We argue that the (anti)quark suppression included in this approach may be responsible for reduced (anti)baryon-to-meson ratios observed in heavy-ion collisions at energies available at the CERN Large Hadron Collider.

I. INTRODUCTION

Relativistic heavy-ion collisions open the possibility to create in the laboratory strongly interacting matter under extreme conditions of high excitation energies and particle densities. One of the central questions is how the initial highly nonequilibrated system evolves to a state of partial thermodynamic equilibrium. There exist several models which describe the initial state in terms of nonequilibrium parton cascades [1,2], minijets [3], color glass condensate [4], coherent chromofields [5,6], etc.

Relatively large gluon-gluon cross sections lead to the idea [7] that the gluonic components of colliding nucleons interact more strongly than the quark-antiquark ones. As demonstrated in Ref. [8], strong nonequilibrium effects in the gluonic sector persist only for a short time $\sim 1/Q_s$, where $Q_s \simeq 1$–2 GeV is the so-called saturation scale [9], but at later times the system reaches a state of a partial thermodynamic equilibrium. The two-step equilibration scenario of the quark-gluon plasma (QGP) was proposed in [10–12]. It was assumed that the gluon thermalization takes place at the proper time $\tau_g < 1$ fm/c and the (anti)quarks equilibration occurs at $\tau_{\rm th} > \tau_g$. The estimates of Ref. [2] show that $\tau_{\rm th}$ can be of the order of 5 fm/c. Later, such a scenario for heavy-ion collisions was considered by several authors; see, e.g., [13–22]. Recently the *pure glue* scenario for the initial state of Pb + Pb collisions at Relativistic Heavy Ion Collider (RHIC) and Large Hadron Collider (LHC) energies was proposed in [23,24].

In this paper we describe the evolution of QGP produced in central heavy-ion collisions by using one-dimensional scaling hydrodynamics. In addition to the chemically equilibrated system we also consider a pure glue initial scenario, in which the QGP contains no quarks and antiquarks at the initial state

of its evolution. Below we introduce the effective number of quark degrees of freedom and study the sensitivity of system evolution to the chemical equilibration time. Special attention is paid to the entropy production in this chemically nonequilibrium scenario. It is commonly accepted that an additional entropy can be created due to dissipative processes which are usually described in the framework of viscous hydrodynamics. In the present work, a different mechanism of entropy production is investigated: we show that it may increase during chemically nonequilibrium expansion of matter even in the ideal hydrodynamics. Earlier the role of chemically nonequilibrium effects in entropy evolution of purely hadronic systems was considered in Refs. [25,26], but without a quantitative analysis of the total entropy change.

The paper is organized as follows: In Sec. II we study thermodynamic functions of a chemically undersaturated QGP (uQGP) at different temperatures and quark fugacities. We obtain explicit relations for relative entropy growth in different scenarios of the system evolution. In Sec. III we formulate a simplified model for describing the hydrodynamic evolution of uQGP in heavy-ion collisions. In Sec. IV we present our numerical results and analyze their sensitivity to chemical equilibration time. The summary and outlook are given in Sec. V. Some preliminary results of this paper were presented in Ref. [24].

II. THERMODYNAMICS OF CHEMICALLY UNDERSATURATED QGP

Below we describe the QGP matter produced in heavy-ion collisions by the equation of state (EoS) of an ideal gluon-quark-antiquark gas. It is assumed that gluons are in

full thermodynamic equilibrium while quarks and antiquarks are in thermal equilibrium, but not necessarily in chemical equilibrium. In this section the thermodynamic functions of chemically nonequilibrium QGP are obtained, and the chemical equilibration process in a static box is investigated.

A. Thermodynamic functions of uQGP

In the following we consider systems with equal numbers of quarks and antiquarks. In the pure glue initial scenario there is undersaturation of (anti)quarks, hence, their chemical potentials are negative:

$$\mu_q = \mu_{\bar{q}} \equiv \mu < 0. \tag{1}$$

We define the (anti)quark fugacity as

$$\lambda = e^{\mu/T} < 1. \tag{2}$$

The phase-space distribution functions of the ideal gas of massless quarks and antiquarks can be written as[1]

$$f_q(\boldsymbol{p}) = f_{\bar{q}}(\boldsymbol{p}) = \frac{g_q}{(2\pi)^3}\left[\exp\left(\frac{p-\mu}{T}\right)+1\right]^{-1}$$

$$= \frac{g_q \lambda}{(2\pi)^3}\left[\exp\left(\frac{p}{T}\right)+\lambda\right]^{-1}, \tag{3}$$

where $\boldsymbol{p}$ is the (anti)quark three–momentum in the fluid's rest frame and the degeneracy factor $g_q = 2 N_c N_f$, where $N_c = 3$ is the number of colors, and N_f is the number of quark flavors. Unless stated otherwise, we assume that $N_f = 3$.

The Fermi-Dirac integral of the nth order is defined as

$$\varphi_n(\lambda) = \frac{\lambda}{\Gamma(n)}\int_0^\infty \frac{dx\, x^{n-1}}{e^x+\lambda} = \sum_{k=1}^\infty (-1)^{k+1}\lambda^k\, k^{-n}. \tag{4}$$

It is easy to show that $\varphi_n' = \varphi_{n-1}/\lambda$, and, therefore, $\varphi_n(\lambda)$ monotonically increases in the interval $\lambda \in [0;1]$. Instead of φ_n it is useful to introduce the function

$$\Lambda_n(\lambda) \equiv \frac{\varphi_n(\lambda)}{\varphi_n(1)} = \frac{\lambda - \lambda^2\, 2^{-n} + \lambda^3\, 3^{-n} - \cdots}{1 - 2^{-n} + 3^{-n} - \cdots}, \tag{5}$$

which is normalized to unity at $\lambda = 1$. The functions λ, Λ_3, and Λ_4 are compared in Fig. 1. It is seen that they are very close to each other. Thus, one can safely use the approximate relations $\Lambda_4 \simeq \lambda$ and $\Lambda_3 \simeq \lambda$.

Using Eq. (3), one can represent the partial energy density ε_q and pressure P_q of quarks and antiquarks as functions of T and μ:

$$\varepsilon_q = 3P_q = \int d^3p\,(f_q+f_{\bar{q}})p$$

$$= \frac{\lambda g_q}{\pi^2}\int_0^\infty dp\, p^3\left(e^{p/T}+\lambda\right)^{-1}$$

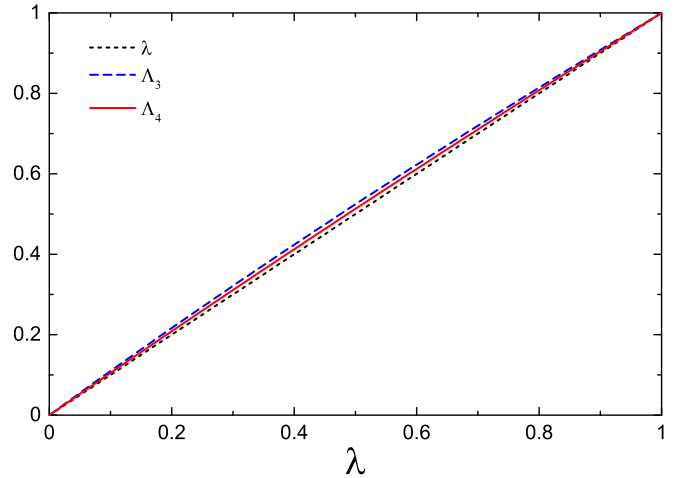$$= \frac{6 g_q}{\pi^2}T^4\varphi_4(\lambda) = 3P_q^{\text{eq}}(T)\,\Lambda_4(\lambda), \tag{6}$$

FIG. 1. The functions Λ_3 and Λ_4 versus the quark fugacity λ.

where

$$P_q^{\text{eq}}(T) = \frac{2 g_q}{\pi^2}T^4\varphi_4(1) = \frac{7\pi^2}{60}N_f T^4 \tag{7}$$

is the chemically equilibrated value of the (anti)quark pressure at $\lambda = 1$. Here and below we use the superscript "eq" to mark characteristics of chemically equilibrated matter.

By using Eq. (6), one can calculate the total density of quarks and antiquarks,

$$n_q = \left(\frac{\partial P_q}{\partial \mu}\right)_T = \frac{2 g_q}{\pi^2}T^3\varphi_3(\lambda) = n_q^{\text{eq}}(T)\,\Lambda_3(\lambda), \tag{8}$$

where

$$n_q^{\text{eq}}(T) = \frac{2 g_q T^3}{\pi^2}\varphi_3(1) \tag{9}$$

is the chemically equilibrated value of the (anti)quark density. The above equations show that Λ_3 and Λ_4 are, respectively, the suppression factors of density and energy density of (anti)quarks in the hot glue initial scenario as compared to the equilibrium case.[2] Using Eq. (2) one can evaluate the contribution of (anti)quarks to the entropy density,[3]

$$s_q = \left(\frac{\partial P_q}{\partial T}\right)_\mu = \frac{4P_q}{T} + n_q \ln(\lambda^{-1}). \tag{10}$$

Neglecting deviations from chemical equilibrium for gluons we get the following relations for gluonic parts of energy density ε_g, pressure P_g, and entropy density s_g:

$$\varepsilon_g = 3P_g = \frac{3}{4}s_g T = \frac{8\pi^2}{15}T^4. \tag{11}$$

Adding the contributions of gluons, quarks, and antiquarks gives the expressions for the total energy density ε, pressure

---

[1] Units $\hbar = c = k = 1$ are used throughout the paper.

[2] As follows from the relations $\Lambda_3 \simeq \Lambda_4 \simeq \lambda$, both these suppression factors are approximately equal to the quark fugacity λ.

[3] The same relation follows from the thermodynamic identity $T s_q = \varepsilon_q + P_q - \mu\, n_q$.

P, and entropy density s density of the uQGP:

$$\varepsilon = 3P = \frac{8\pi^2}{15} T^4 [1 + \alpha\Lambda_4(\lambda)], \qquad (12)$$

$$s = \frac{32\pi^2}{45} T^3 [1 + \alpha\Lambda_4(\lambda) - \beta\Lambda_3(\lambda)\ln\lambda], \qquad (13)$$

where

$$\alpha = \frac{7g_q}{64} \simeq 0.656\, N_f, \quad \beta = \frac{45\, g_q}{16\,\pi^4} \varphi_3(1) \simeq 0.156\, N_f. \qquad (14)$$

In the last equality of Eq. (14) we use the relation $\varphi_3(1) = 3\,\xi(3)/4$, where $\xi(3) \simeq 1.20\,2$ is the Riemann zeta function $\xi(x) = \sum_{k=1}^{\infty} k^{-x}$ at $x = 3$.

B. Equilibration in a box

Let us consider first the evolution of a homogeneous, chemically nonequilibrium QGP in a static box of volume V. We assume that initially this plasma contains only gluons (i.e., $\lambda = 0$) at the temperature $T = T_0$. In the absence of the partons' exchange with the box exterior, the system should approach the equilibrium state with $\lambda = 1$ at large times. In the general case, the energy and entropy densities of the system in intermediate states are functions of both T and λ. The time evolution of temperature depends on boundary conditions which in turn determine the type of a thermodynamic process. We consider two limiting cases: the isothermal process ($T = T_0$), which requires some heat transfer from outside, and the process with fixed energy ($\varepsilon = \varepsilon_0$). The second case corresponds to a thermally isolated system without any heat exchange.[4]

From Eq. (13) one gets the expression for the ratio of the total entropy $S = sV$ with respect to its initial value:

$$\frac{S}{S_0} = \left(\frac{T}{T_0}\right)^3 (1 + \alpha\Lambda_4 - \beta\Lambda_3\ln\lambda). \qquad (15)$$

Here and below we omit arguments λ in the functions Λ_3 and Λ_4. In the isothermal case we obtain

$$\frac{S}{S_0} = 1 + \alpha\Lambda_4 - \beta\Lambda_3\ln\lambda \xrightarrow[\lambda\to 1]{} 1 + \alpha \quad (T = T_0). \qquad (16)$$

Note that the gluon fraction of entropy (the first term in the right-hand side) does not change with time in the isothermal process. One can see that the relative increase of entropy is proportional to the number of quark flavors N_f.

The fixed-energy case is more complicated. As one can see from Eq. (12), the systems cools down during the process of chemical equilibration:

$$T = T_0 (1 + \alpha\Lambda_4)^{-1/4} \quad (\varepsilon = \varepsilon_0). \qquad (17)$$

---

[4]It will be shown that the relative change of the total entropy as a function of λ coincides in this case with the corresponding quantity for a Bjorken-like expanding QGP.
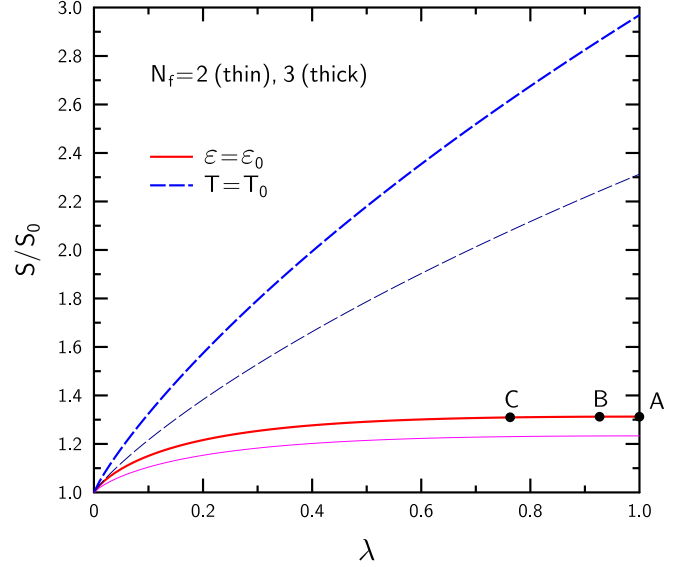

FIG. 2. Relative increase of entropy of uQGP with respect to the pure glue initial state as a function of quark fugacity λ. Solid (dashed) lines correspond to box calculations with constant energy density (temperature). Thin and thick lines are calculated for the quark flavor numbers 2 and 3, respectively. Dots correspond to freeze-out states, estimated from Bjorken hydrodynamic analysis of central Pb + Pb collisions at LHC energy (see below).

Substituting this temperature into Eq. (15) gives the following result:

$$\frac{S}{S_0} = \frac{1 + \alpha\Lambda_4 - \beta\Lambda_3\ln\lambda}{(1 + \alpha\Lambda_4)^{3/4}} \xrightarrow[\lambda\to 1]{} (1 + \alpha)^{1/4} \quad (\varepsilon = \varepsilon_0). \qquad (18)$$

From the comparison of Eqs. (16) and (18) one can see that the relative increase of entropy is smaller in the second case. The asymptotic values of S/S_0 are equal in this case to 23% and 31% (approximately) for $N_f = 2$ and 3, respectively.

Figure 2 shows the results of numerical calculations of S/S_0 for both considered cases. In Fig. 3 we consider in more details the system equilibration at $\varepsilon = \varepsilon_0$. One can see that in this case the fraction of entropy contained in gluons decreases with time; however, this decrease is more than compensated by a rising contribution of $q\bar{q}$ pairs.

III. EVOLUTION OF UNDERSATURATED QGP WITHIN THE BJORKEN HYDRODYNAMICS

We consider central Pb + Pb collisions at ultrarelativistic energies of the LHC. Our calculations below are performed under the following assumptions:

Equation of state. The matter produced in the central rapidity region at LHC energies has a nearly vanishing net baryon density. To describe this matter we apply the EoS of an ideal gas of massless gluons, quarks, and antiquarks obtained in Sec. II A. According to Eq. (12), this EoS can be written in the Stefan–Boltzmann form, $\varepsilon = 3P = \sigma T^4$, where the coefficient $\sigma \propto 1 + \alpha\Lambda_4(\lambda)$. The first and second terms in this
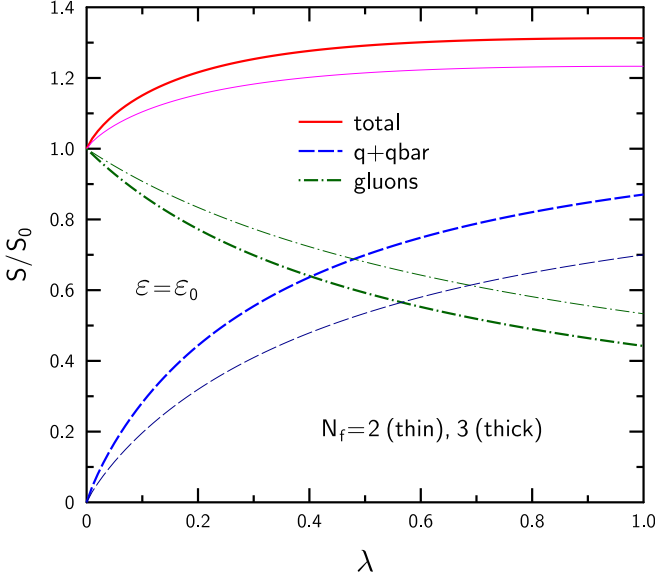
FIG. 3. Entropy ratios in uQGP with respect to the pure glue initial state as functions of quark fugacity λ. Thin and thick lines correspond to box calculations with constant energy density for the quark flavor numbers 2 and 3, respectively. The dashed (dash-dotted) lines give contributions of $q\bar{q}$ pairs (gluons) to the total entropy ratios (the solid curves).

expression describe, respectively, the contributions of gluons[5] and $q\bar{q}$ pairs. The quantity Λ_4 is the quark suppression factor, approximately equal to the (anti)quark fugacity λ.

Bjorken hydrodynamics. Space-time evolution of uQGP is described by the ideal relativistic hydrodynamics. Corresponding equations of motion can be written as

$$\frac{\partial T^{\mu\nu}}{\partial x^\nu} = 0, \tag{19}$$

where

$$T^{\mu\nu} = (\varepsilon + P)\, u^\mu u^\nu - P g^{\mu\nu} \tag{20}$$

is the energy-momentum tensor, u^μ is the flow four-velocity, and $g^{\mu\nu}$ is the diagonal metric tensor with $g^{00} = -g^{11} = -g^{22} = -g^{33} = 1$.

Below we neglect the transverse motion of matter created in a nuclear collision. The center-of-mass frame will be used with the longitudinal axis z taken along the beam direction. Following the Bjorken model [27], we assume that a thermally (but not necessary chemically) equilibrated QGP has been created at $\tau = \tau_0, r_\perp = \sqrt{x^2 + y^2} < R_A$, where $\tau = \sqrt{t^2 - z^2}$ is the proper time of a fluid element and R_A is the geometrical radius of initial nuclei. We consider only the (1+1)-dimensional, boost-invariant solution of hydrodynamic equations which satisfies the conditions [27–32]

$$u^\mu = \frac{1}{\tau}(t, \mathbf{0}, z)^\mu, \quad \varepsilon = \varepsilon(\tau), \quad P = P(\tau). \tag{21}$$

---

[5]As already mentioned, we neglect deviations from chemical equilibrium for gluons during the whole process of the uQGP evolution.

Using these relations one can show that Eqs. (19) and (20) are reduced to the equation

$$\frac{d\varepsilon}{d\tau} + \frac{\varepsilon + P}{\tau} = 0. \tag{22}$$

Substituting the relation $P = \varepsilon/3$ in Eq. (22) one obtains

$$\varepsilon = \varepsilon(\tau_0)\left(\frac{\tau_0}{\tau}\right)^{4/3}, \tag{23}$$

where the parameter τ_0 corresponds to the initial proper time of the hydrodynamic expansion.

Entropy increase. For the boost-invariant Bjorken expansion, the total entropy per unit space-time rapidity can be expressed as [33]

$$\frac{dS(\tau)}{d\eta} = \pi\, R_A^2\, s(\tau)\, \tau, \tag{24}$$

where the space-time rapidity η is defined as $\eta = \tanh^{-1}(z/t)$. Because of the boost invariance, $dS/d\eta$ does not depend on η within the Bjorken model. In the case of chemical equilibrium, i.e., when $\lambda = 1$, the entropy density (in the net baryon-free matter) $s = (\varepsilon + P)/T$ is inversely proportional to τ:

$$s(\tau) = \frac{s_0 \tau_0}{\tau}, \tag{25}$$

where $s_0 = s(\tau_0)$. In this particular case Eqs. (23) and (25) are equivalent. From Eqs. (24) and (25) one can see that $dS/d\eta$ is conserved during the hydrodynamical expansion of chemically equilibrated matter. In a general case of a time-dependent λ, Eqs. (23) and (25) are not equivalent, and the entropy $dS/d\eta$ is not conserved but increases during the hydrodynamic expansion (see below).

Freeze-out condition. We assume that the Bjorken solution is valid until the "freeze-out" (hyper)surface $\tau = \tau_f$. Below we analyze a purely central Pb + Pb collisions at the LHC bombarding energy of $\sqrt{s_{\rm NN}} = 2.76$ TeV. The freeze-out time τ_f will be determined by the condition

$$T(\tau_f) = 156 \text{ MeV}. \tag{26}$$

Such a temperature value has been extracted [34] from the thermal fit of hadron ratios observed in the considered reaction.

To get numerical estimates we use the approximate relation [35] between the total entropy per unit space-time rapidity and the rapidity density of pions:

$$\frac{dS(\tau_f)}{d\eta} = \nu \left.\frac{dN_\pi}{dy}\right|_{y=\eta} = \pi R_A^2\, s(\tau_f)\, \tau_f, \tag{27}$$

where ν is the entropy per pion at the freeze-out stage of a heavy-ion collision. Note that commonly used value $\nu = 3.6$ [11] does not take into account that a large part of entropy is carried by heavy mesons ($\rho, \omega, \ldots$) and baryon-antibaryon pairs ($N, \overline{N}, \Delta, \overline{\Delta}, \ldots$). The decay of hadronic resonances gives a significant fraction of observed pions. Our calculations within the hadron resonance gas model [36,37] show that $\nu \simeq 6.3$ at $T \simeq 156$ MeV and vanishing net baryon density. Using experimental data of Ref. [38] we obtain that $dN_\pi/dy|_{y=0} \simeq 2700$. Substituting $R_A \simeq 6.5$ fm and $\nu = 6.3$

into Eq. (27) we get the estimate

$$\frac{dS(\tau_f)}{d\eta} \simeq 1.7 \times 10^4, \qquad (28)$$

which is used in our numerical calculations (see next section).

IV. NUMERICAL RESULTS

We compare two scenarios: the equilibrium QGP with the quark fugacity $\lambda = 1$ and the chemically nonequilibrium uQGP with $\lambda = \lambda(\tau) < 1$. In the second scenario we assume that $\lambda(\tau_0) \ll 1$ and $\lambda \to 1$ at later times. Below we use the parametrization

$$\lambda(\tau) = 1 - \exp\left(\frac{\tau_0 - \tau}{\tau_*}\right), \qquad (29)$$

where τ_* is the model parameter characterizing the quark chemical equilibration time. Calculations of different authors gives different estimates for τ_* ranging from $\tau_* \sim 1$ fm/c [22] to $\tau_* \sim 5$ fm/c [2]. One should have in mind that this parameter may depend on the combination of nuclei and the bombarding energy. We expect that τ_* will be larger for peripheral events and lighter combinations of nuclei. Figure 1 shows the time dependence of λ for several values of the parameters τ_0 and τ_*. At small initial times, $\lambda(\tau)$ is only slightly sensitive to τ_0. The chemically equilibrated case ($\lambda = 1$) can be obtained at $\tau_* \to 0$. The case of a pure glue plasma corresponds to the limit $\tau_* \to \infty$.

Let us consider in more details the dynamics of the uQGP in the Bjorken model. Using Eqs. (23) and (12), one gets the relations $\varepsilon \propto T^4(1 + \alpha\Lambda_4) \propto \tau^{-4/3}$. This gives the following equation for temperature at $\tau \geqslant \tau_0$

$$T = T_0\left(\frac{\tau_0}{\tau}\right)^{1/3}(1 + \alpha\Lambda_4)^{-1/4}. \qquad (30)$$

The explicit expression for $\Lambda_4(\tau)$ is obtained by substituting (29) into Eq. (5) with $n = 4$. As compared to the evolution of uQGP in the static box [see Eq. (17)], the temperature contains the additional factor $(\tau_0/\tau)^{1/3}$. A stronger cooling in the expanding plasma occurs due to the work of pressure gradients which accelerate fluid elements in the Bjorken model.

It is useful to rewrite Eq. (13) in the form

$$s = s_0\left(\frac{T}{T_0}\right)^3(1 + \alpha\Lambda_4 - \beta\Lambda_3 \ln\lambda), \qquad (31)$$

where s_0 is the initial value of the entropy density. The latter is given by the first factor in the right-hand side (r.h.s.) of (13) taken at $T = T_0$. Using Eqs. (24), (30), and (31) we get the equation for the total entropy of the QGP per unit space-time rapidity:

$$\frac{dS(\tau)}{d\eta} = \frac{dS(\tau_0)}{d\eta}\frac{1 + \alpha\Lambda_4 - \beta\Lambda_3 \ln\lambda}{(1 + \alpha\Lambda_4)^{3/4}}. \qquad (32)$$

The first factor in the r.h.s. is given by Eq. (24) with the replacement $s\tau \to s_0\tau_0$. As seen from the comparison with Eq. (18), we get the same entropy enhancement factor (as a function of λ) as for the box equilibration in the fixed-energy case.

Substituting $\tau = \tau_f$ into (30) and (32) and using Eqs. (26) and (28) gives two coupled equations for determining the initial temperature T_0 and the freeze-out time τ_f. The results of the calculation for several values of τ_0 and τ_* are given below (we take the same parameters as in Fig. 4 and consider the number of flavors $N_f = 3$). For comparison we also make calculations within the chemically equilibrated scenario.[6] The values of T_0, τ_f calculated for all considered combinations of parameters are shown in Table I. The last two columns give the fugacity and the chemical potential of quarks at freeze-out. One can see that in all cases the initial temperature significantly exceeds the equilibrium value.

A more detailed information is contained in Figs. 5 and 6. The time dependence of temperature calculated from Eq. (30) is shown in Fig. 5. One can see that the deviation from equilibrium is most significant at the early stage, and the pure glue initial scenario predicts a higher temperature at any τ. Consequently, while there is a smaller amount of quarks during the evolution of the uQGP than in the equilibrium case, they are generally hotter. Note that a twofold increase of the equilibration parameter τ_*, from 5 to 10 fm/c, only slightly

---

[6]In this case we take the same values of τ_0 and the same pion multiplicity and temperature at freeze-out as for uQGP.
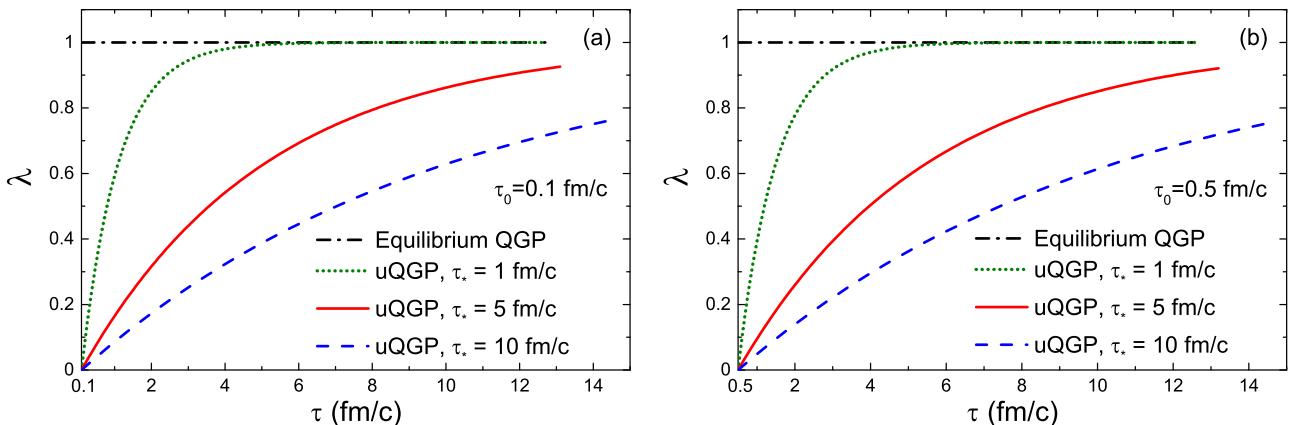

FIG. 4. The quark fugacity λ as a function of proper time τ for two evolution scenarios with (a) $\tau_0 = 0.1$ fm/c and (b) $\tau_0 = 0.5$ fm/c. The dotted, solid, and dashed lines correspond to uQGP, with parameters $\tau_* = 1$ fm/c, 5 fm/c, and 10 fm/c, respectively.

TABLE I. The values of initial temperature T_0, freeze-out proper time τ_f, quark fugacity λ, and quark chemical potential μ at $\tau = \tau_f$ for all considered cases.

τ_0 (fm/c)	τ_* (fm/c)	τ_f^{eq} (fm/c)	T_0^{eq} (MeV)	τ_f (fm/c)	T_0 (MeV)	λ_f	μ_f (MeV)
0.1	1	12.7	779	12.7	1022	1.00	0
0.1	5	12.7	779	13.2	1023	0.927	−12
0.1	10	12.7	779	14.5	1024	0.763	−42
0.5	1	12.7	456	12.7	598	1.00	0
0.5	5	12.7	456	13.2	598	0.921	−13
0.5	10	12.7	456	14.6	599	0.756	−44

changes the cooling law $T = T(\tau)$ of the undersaturated matter.

The evolution of the total entropy per unit space-time rapidity calculated using Eq. (32) is shown in Fig. 6. One can see that the entropy in the chemically nonequilibrium scenario increases gradually with time, and about 25% of the final value (28) is generated during the hydrodynamic expansion. Our calculations show that the characteristic time of the entropy increase is of the order of τ_*. However, the total amount of produced entropy only weakly changes with τ_*. This is also seen in Fig. 2, where we show points A, B, and C (these points correspond, respectively, to the values of λ_f from the first three lines of Table I).

As seen from Fig. 4 and Table I, the quark fugacity λ remains smaller than unity at the freeze-out hypersurface $\tau = \tau_f$ in the chemically nonequilibrium scenario. This implies the suppression of quarks and antiquarks as compared to the equilibrium QGP even at the hadronization stage. Such a behavior may influence the hadron composition measured in central Pb + Pb collisions at LHC energies. Note that the hadron resonance gas model [39–41] cannot explain the observed chemical composition of hadrons observed [42] in these collisions. In particular, the measured (anti)proton-to-pion ratios are noticeably smaller than their equilibrium values for baryon-free matter. Calculations which allow deviations from the hadron equilibrium scenario are, thus, necessary.
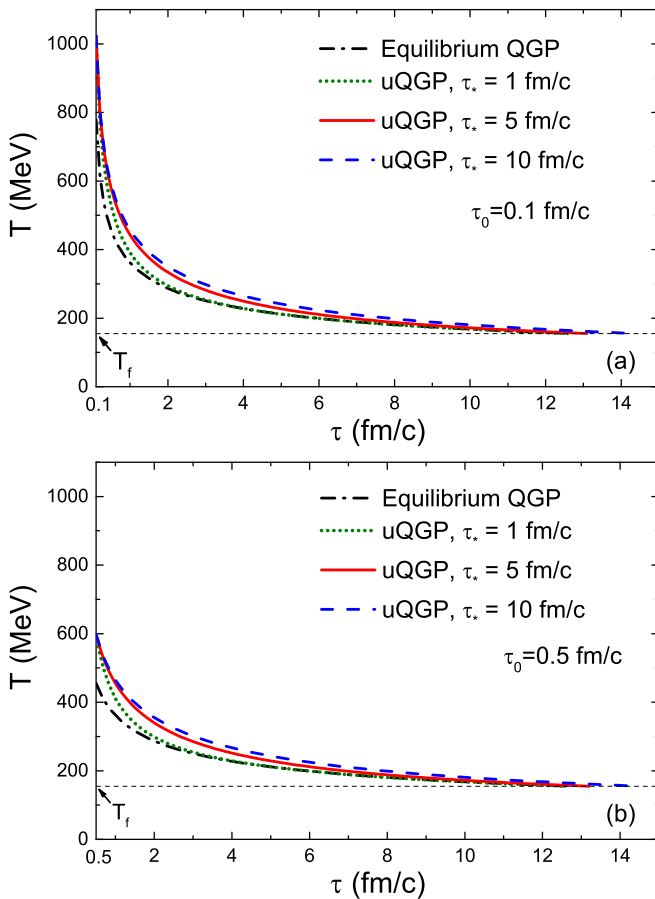

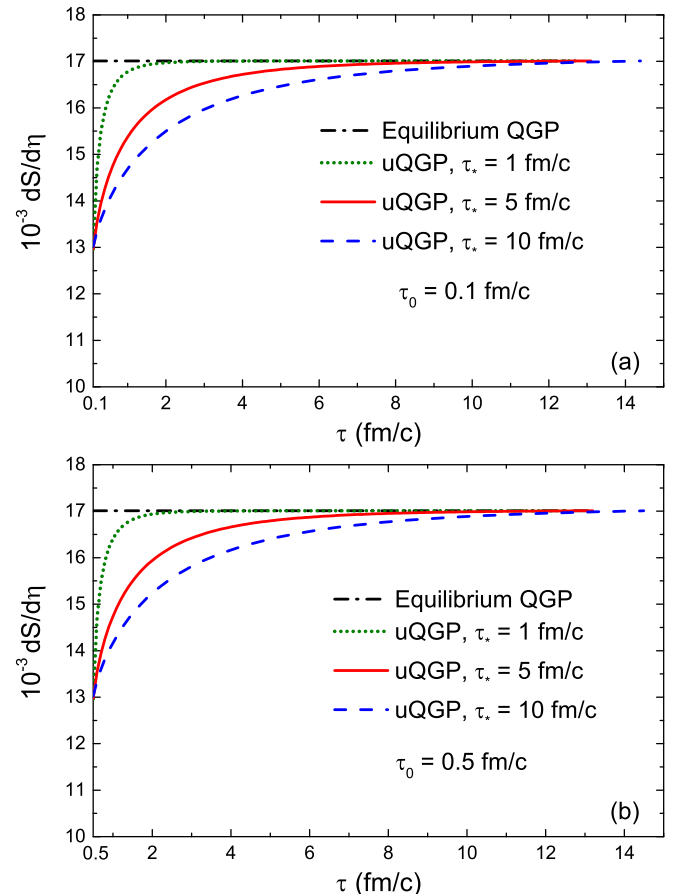FIG. 5. Same as Fig. 4, but for temperature as a function of τ.

FIG. 6. Same as Fig. 4, but for entropy per unit space-time rapidity.

Several theoretical models have been suggested to explain deviations from chemical equilibrium observed at LHC. Baryon suppression due to inelastic collisions of hadrons at post freeze-out stage of a nuclear collision has been studied in [43]. Possibility of pion enhancement due to positive pion chemical potentials was also investigated [44]. In the present paper we propose an alternative explanation of the observed suppression of the p/π and $\overline{p}/\pi$ ratios. Indeed, according to the constituent quark structure of protons, antiprotons, and pions, one can estimate the suppression factor for both these ratios as $\lambda_f^3/\lambda_f^2 = \lambda_f$. The latter can be noticeably below unity in undersaturated matter (see the corresponding column of Table I). The same estimate can be obtained in the parton recombination model [45] with chemically nonequilibrium effects as well as in the statistical hadronization approach [46]. The comparison of RHIC and LHC data shows [42] that (anti)baryon-to-pion ratios are less suppressed at RHIC. This may be caused by a slower evolution of the fireball at lower incident energies.

Another mechanism was proposed in Refs. [26,36], where the p/π suppression is explained by annihilation of baryon-antibaryon pairs in dense hadronic matter created in nuclear collisions. According to Ref. [36], the p/π ratios observed in central collisions can be reproduced if the annihilation persists until the temperature drops to 100–120 MeV. Due to faster expansion and cooling of matter in peripheral events, one can expect stronger annihilation effects in more central collisions. However, the ALICE data [42] reveal only small variations of the p/π ratio as a function of centrality. This discrepancy might be resolved by assuming some initial undersaturation of baryon-to-meson ratios, which increases with impact parameter.[7] The latter assumption is rather natural because of reduced lifetimes of the deconfined phase in more peripheral events. We plan to extend the approach developed in Refs. [26,36] for chemically nonequilibrium initial states in nuclear collisions.

V. CONCLUSIONS AND OUTLOOK

We have investigated the dynamical evolution of deconfined matter with changing chemical composition as expected in heavy-ion collisions at LHC energies. Two scenarios have been considered in details. The first one assumes that initially the system is composed exclusively of gluons, and later on quark-antiquark pairs are created during the characteristic time of 1–5 fm/c. The second scenario assumes that the equilibrated QGP exists already at the initial stage. The model parameters are chosen in such a way that the final pion multiplicity in both cases is equal to the observed value for central Pb + Pb collisions. We predict that in the nonequilibrium scenario about 25% of final entropy is generated due to chemical equilibration of plasma. We want to stress that this effect of

entropy production is present in ideal hydrodynamics and it is attributed to increasing number of degrees of freedom. This is different from the case of entropy production via dissipative processes which are determined by transport coefficients and usually modeled by the viscous hydrodynamics. Obviously, the inclusion of chemically nonequilibrium effects may require modification of the viscosity coefficients extracted from the fit of collective flow observables [49,50].

In the present work we do not develop any full-fledged formalism to describe the pure glue initial scenario. Ideally, one would like to determine the dynamical evolution of matter created in heavy-ion collisions directly from experimental data. That would require using a model working in a reverse way, starting from the measured data, such as identified particle momentum spectra, and then proceeding backwards in time. Reversing a dynamical evolution in an ideal (1+1)-dimensional hydrodynamics has been performed in Ref. [51]. Note, however, that uncertainties in the final state measured in detectors increase when going backwards in time. Furthermore, irreversible processes, associated with viscosity, as well as with particle production out of equilibrium, as discussed in this paper, lead to an increase of entropy and further reduce the accuracy of this back-tracing procedure.

A crucial test of the pure glue initial scenario may be provided by the electromagnetic probes, i.e., by emission of thermal photons and dileptons. This study will be presented in a forthcoming publication (our preliminary results are given in Ref. [24]). We also plan to perform a more realistic calculation within a (3+1)-dimensional hydrodynamic model which takes into account the transverse motion of matter. Then one can analyze the sensitivity of photon and hadron observables to chemically nonequilibrium effects at early stages, and to violation of Bjorken scaling at later stages of a heavy-ion collision. The calculations can be made even more realistic by introducing additional rate equations describing the space-time evolution of quark and gluon densities (see, e.g., [13,16,21]).

We are also going to study in more detail dynamics of the first-order phase transition as predicted in the pure gluodynamics. In particular, it will be interesting to study influence of this phase transition on flow observables (see Refs. [52,53]) . Another interesting possibility is supercooling and overheating processes associated with the deconfinement phase transition [54,55].

---

[7]It is interesting that underpopulation of (anti)baryons at the posthadronization stage of nuclear collisions has been considered in Refs. [47,48] within a model which takes into account the production and decay of Hagedorn resonances.

[1] X.-N. Wang and M. Gyulassy, Phys. Rev. D **44**, 3501 (1991).

[2] Z. Xu and C. Greiner, Phys. Rev. C **71**, 064901 (2005).

[3] K. J. Eskola and K. Kajantie, Z. Phys. C **75**, 515 (1997).

[4] L. D. McLerran and R. Venugopalan, Phys. Rev. D **49**, 2233 (1994).

[5] V. K. Magas, L. P. Csernai, and D. D. Strottman, Phys. Rev. C **64**, 014901 (2001).

[6] I. N. Mishustin and J. I. Kapusta, Phys. Rev. Lett. **88**, 112501 (2002).

[7] L. van Hove and S. Pokorski, Nucl. Phys. B **86**, 243 (1975).

[8] J.-P. Blaizot, F. Gelis, J. Liao, L. McLerran, and R. Venugopalan, Nucl. Phys. A **904–905**, 829c (2013).

[9] L. V. Gribov, E. M. Levin, and M. G. Ryskin, Phys. Rep. **100**, 1 (1983).

[10] S. Raha, Phys. Scr. **T32**, 180 (1990).

[11] E. Shuryak, Phys. Rev. Lett. **68**, 3270 (1992).

[12] Jan-e Alam, S. Raha, and B. Sinha, Phys. Rev. Lett. **73**, 1895 (1994).

[13] T. S. Biró, E. van Doorn, B. Müller, M. H. Thoma, and X.-N. Wang, Phys. Rev. C **48**, 1275 (1993).

[14] M. Strickland, Phys. Lett. B **331**, 245 (1994).

[15] C. T. Traxler and M. H. Thoma, Phys. Rev. C **53**, 1348 (1996).

[16] D. M. Elliott and D. H. Rischke, Nucl. Phys. A **671**, 583 (2000).

[17] D. Dutta, S. V. S. Sastry, A. K. Mohanty, K. Kumar, and R. K. Choudhury, Nucl. Phys. A **710**, 415 (2002).

[18] F. Gelis, H. Niemi, R. V. Ruuskanen, and S. S. Räsänen, J. Phys. G: Nucl. Part. Phys. **30**, S1031 (2004).

[19] F. Scardina, M. Colonna, S. Plumari, and V. Greco, Phys. Lett. B **724**, 296 (2013).

[20] F.-M. Liu and S.-X. Liu, Phys. Rev. C **89**, 034906 (2014).

[21] A. Monnai, Phys. Rev. C **90**, 021901 (2014).

[22] M. Ruggieri, S. Plumari, F. Scardina, and V. Greco, Nucl. Phys. A **941**, 201 (2015).

[23] H. Stöcker *et al.*, J. Phys. G: Nucl. Part. Phys. **43**, 015105 (2016).

[24] H. Stöcker *et al.*, Astron. Nachr. **336**, 744 (2015); arXiv:1509.07682.

[25] H. Bebie, P. Gerber, J. L. Goity, and H. Leutwyler, Nucl. Phys. B **378**, 95 (1992).

[26] Y. Pan and S. Pratt, Phys. Rev. C **89**, 044911 (2014).

[27] J. D. Bjorken, Phys. Rev. D **27**, 140 (1983).

[28] R. C. Hwa, Phys. Rev. D **10**, 2260 (1974).

[29] F. Cooper, G. Frye, and E. Schonberg, Phys. Rev. D **11**, 192 (1975).

[30] C. B. Chiu, E. C. G. Sudarshan, and K. Wang, Phys. Rev. D **12**, 902 (1975).

[31] C. B. Chiu and K. Wang, Phys. Rev. D **12**, 272 (1975).

[32] M. I. Gorenstein, Yu. M. Sinyukov, and V. I. Zhdanov, Phys. Lett. B **71**, 199 (1977).

[33] L. M. Satarov, I. N. Mishustin, A. V. Merdeev, and H. Stöcker, Phys. Rev. C **75**, 024903 (2007).

[34] J. Stachel, A. Andronic, P. Braun-Munzinger, and K. Redlich, J. Phys. Conf. Ser. **509**, 012019 (2014).

[35] R. C. Hwa and K. Kajantie, Phys. Rev. D **32**, 1109 (1985).

[36] L. M. Satarov, I. N. Mishustin, and W. Greiner, Phys. Rev. C **88**, 024908 (2013).

[37] V. Vovchenko, D. V. Anchishkin, and M. I. Gorenstein, Phys. Rev. C **91**, 024905 (2015).

[38] E. Abbas *et al.* (ALICE Collaboration), Phys. Lett. B **726**, 610 (2013).

[39] J. Cleymans, H. Oeschler, K. Redlich, and S. Wheaton, Phys. Rev. C **73**, 034905 (2006).

[40] A. Andronic, P. Braun-Munzinger, and J. Stachel, Nucl. Phys. A **772**, 167 (2006).

[41] A. Andronic, P. Braun-Munzinger, and J. Stachel, Phys. Lett. B **673**, 142 (2009).

[42] B. Abelev *et al.* (ALICE Collaboration), Phys. Rev. C **88**, 044910 (2013).

[43] F. Becattini, M. Bleicher, E. Grossi, J. Steinheimer, and R. Stock, Phys. Rev. C **90**, 054907 (2014).

[44] V. Begun and W. Florkowski, Phys. Rev. C **91**, 054909 (2015).

[45] R. J. Fries, B. Müller, C. Nonaka, and S. A. Bass, Phys. Rev. Lett. **90**, 202303 (2003).

[46] M. Petráň, J. Letessier, V. Petráček, and J. Rafelski, Phys. Rev. C **88**, 034907 (2013).

[47] J. Noronha-Hostler, M. Beitel, C. Greiner, and I. Shovkovy, Phys. Rev. C **81**, 054909 (2010).

[48] J. Noronha-Hostler and C. Greiner, Nucl. Phys. A **931**, 1108 (2014).

[49] P. Romatschke and U. Romatschke, Phys. Rev. Lett. **99**, 172301 (2007).

[50] H. Niemi, G. S. Denicol, P. Huovinen, E. Molnar, and D. H. Rischke, Phys. Rev. Lett. **106**, 212302 (2011).

[51] M. Stephanov and Y. Yin, arXiv:1404.5910.

[52] A. V. Merdeev, L. M. Satarov, and I. N. Mishustin, Phys. Rev. C **84**, 014907 (2011).

[53] Yu. B. Ivanov and A. A. Soldatov, Phys. Rev. C **91**, 024914 (2015); **91**, 024915 (2015).

[54] C. Herold, M. Nahrgang, I. Mishustin, and M. Bleicher, Nucl. Phys. A **925**, 14 (2014).

[55] J. Steinheimer and J. Randrup, Phys. Rev. Lett. **109**, 212301 (2012).